A single amino acid substitution (H451Y) in Leishmania calcium-dependent kinase SCAMK confers high tolerance and resistance to antimony

Baptiste Vergnes, Elodie Gazanion, Cédric Mariac, Miléna Du Manoir, Lauriane Sollelis, Jose-Juan Lopez-Rubio, Yvon Sterkers, Anne-Laure Bañuls

Title: A single amino acid substitution (H451Y) in *Leishmania* calcium-dependent kinase SCAMK confers high tolerance and resistance to antimony.

Running title: *Leishmania* tolerance and resistance

Authors: Baptiste VERGNES[1*], Elodie GAZANION[1], Cédric MARIAC[2], Miléna DU MANOIR[1], Lauriane SOLLELIS[1], José-Juan LOPEZ-RUBIO[1], Yvon STERKERS[1,3], Anne-Laure BAÑULS[1]

Contact Information: [1] MIVEGEC, IRD, CNRS, Univ. Montpellier, Montpellier, France; [2] DIADE, IRD, Univ. Montpellier, Montpellier, France; [3] Department of Parasitology-Mycology, Faculty of Medicine, University Hospital Center of Montpellier, Univ. Montpellier, Montpellier, France.

Present address: Lauriane Sollelis, Wellcome Centre for Molecular Parasitology, Institute of Infection, Immunity & Inflammation, College of Medical, Veterinary and Life Sciences, University of Glasgow, Glasgow, UK

***Corresponding author:** Baptiste Vergnes Ph.D., UMR MIVEGEC (IRD, CNRS, Univ. Montpellier), 911 Avenue Agropolis, 34394 Montpellier Cedex 5, France. Phone number: +33(0)467416308. Email address: baptiste.vergnes@ird.fr

A final version of this manuscript has been published, please cite:
Baptiste Vergnes, Elodie Gazanion, Cédric Mariac, Miléna Du Manoir, Lauriane Sollelis, José-Juan Lopez-Rubio, Yvon Sterkers, Anne-Laure Bañuls, A single amino acid substitution (H451Y) in Leishmania calcium-dependent kinase SCAMK confers high tolerance and resistance to antimony, Journal of Antimicrobial Chemotherapy, Volume 74, Issue 11, November 2019, Pages 3231–3239, https://doi.org/10.1093/jac/dkz334

Synopsis:

Background: For almost a century, antimonials remain the first-line drugs for the treatment of leishmaniasis. However, little is known about their mode of action and clinical resistance mechanisms.

Objectives: We have previously shown that *Leishmania* nicotinamidase (PNC1) is an essential enzyme for parasite NAD+ homeostasis and virulence *in vivo*. Here, we found that parasites lacking *pnc1* gene (Δ*pnc1*) are hypersusceptible to the active form of antimony (SbIII) and used these mutant parasites to better understand antimony mode of action and resistance.

Methods: SbIII-resistant WT and Δ*pnc1* parasites were selected *in vitro* by stepwise selection method. NAD(H)/NADP(H) dosages and quantitative RT-PCR experiments were performed to explain the susceptibility differences observed between strains. WGS and a marker-free CRISPR/Cas9 base editing approach were used to identify and validate the role of a new resistance mutation.

Results: NAD+ depleted Δ*pnc1* parasites are highly susceptible to SbIII and this phenotype can be rescued by NAD+ precursor of trypanothione precursors supplementation. Δ*pnc1* parasites can become resistant to SbIII by unknown mechanism. WGS revealed a unique amino acid substitution (H451Y) in an EF-hand domain of an orphan calcium-dependent kinase recently named SCAMK. When introduced into a wild type reference strain by base editing, the H451Y mutation allows *Leishmania* parasites to survive at extreme concentrations of SbIII, potentiating the rapid emergence of resistant parasites.

Conclusions: These results establish that *Leishmania* SCAMK is a new central hub of antimony mode of action and resistance development and uncover the importance of drug tolerance mutations in the evolution of parasite drug resistance.

Introduction

Leishmania are protozoan parasites transmitted by sandflies that are responsible for a wide spectrum of human infections ranging from the life-threatening visceral disease to disfiguring mucosal and cutaneous forms[1]. Treatment of leishmaniasis is limited to four main drugs (antimonials, miltefosine, amphotericin B and paromomycin). Alone or in combination, antimonials have been the mainstay of anti-*Leishmania* therapy worldwide for over 70 years. However, our knowledge of antimony mode of action is still partial and the emergence of parasite resistance to antimony in the Indian subcontinent during the last decades has necessitated the use of alternative medications. The active form of antimony (SbIII) is known to target the *Leishmania* redox potential by inducing rapid thiols efflux and inhibiting the NADPH-dependent trypanothione reductase (TR) that maintains the main parasite thiol, trypanothione, in its reduced form[2] (Figure 1a). *Leishmania* resistance to SbIII is generally mediated by drug uptake reduction through the aquaglyceroprotein 1 (AQP1) transporter mutations or down-expression, or by drug efflux/sequestration through the concomitant overexpression of genes involved in the parasite thiol metabolism and of the gene encoding the ATP-binding cassette transporter ABC-C3 (MRPA)[3,4] (Figure 1a). Other transporters of the ABC superfamily also interfere with antimonials drug accumulation, including ABC-C7 (PRP1)[5], ABC-I3[6], ABC-I4[7] or ABC-G2[8]. In addition, it has been shown that a number of intracellular proteins can also modulate the susceptibility of parasites to SbIII when they are overexpressed in experimental strains or clinical isolates. These include heat shock proteins (Hsp23[9], Hsp83[10]), kinase (MAPK1[11]), serine/threonine phosphatase (LinJ.12.0610[12]) or proteins with still unknown functions (ARM56[9], ARM58[9], P299[13]). Overall, these results illustrate that *Leishmania* parasites have multiple strategies to acquire drug resistance and highlight the difficulty to define a conserved molecular marker of antimony resistance.

In a previous work[14], we showed that *Leishmania* parasites are auxotrophic for NAD+ and rely on a salvage pathway to recycle NAD+ precursors from their environment (Figure 1a). The nicotinamidase PNC1 is a central enzyme of this pathway that controls NAD+ homeostasis by hydrolysing nicotinamide (NAm) to nicotinic acid (NA). *Leishmania infantum* parasites in which the *pnc1* gene was disrupted (Δ*pnc1*) are depleted in NAD+ and cannot cause durable infections in mice, making of this enzyme an attractive target for drug development[14,15]. NAD(H), and its derived phosphorylated forms NADP(H), are essential cofactors required for

energy-producing pathways and antioxidant defence in all living cells. They are further key metabolites involved in host-pathogen interactions[16]. Here, we used NAD+ depleted Δ*pnc1* mutant parasites to better understand SbIII mode of action and the mechanisms leading to resistance to this drug. We found that intracellular NAD+ levels can directly modulate the susceptibility of parasites to SbIII and identified the first mutation conferring antimony tolerance and resistance in *Leishmania*.

Materials and Methods

Strains and cultures

The *pnc1* null mutant (Δ*pnc1*) was previously generated by targeted gene replacement in the *L. infantum* (MHOM/MA/67/ITMAP-263) strain[14]. CRISPR/Cas9 genome edition experiments were performed in the *L. major* "Friedlin" reference strain (MHOM/IL/80/Friedlin, LEM3171)[17]. All strains and the derived mutants were maintained as promastigote forms in SDM79 medium supplemented with 10% FBS, penicillin/streptomycin and hemin (5 mg/L) (complete medium). Potassium antimonyl tartrate trihydrate (SbIII), L-Glutathione reduced (GSH), N-Acetyl-L-cysteine (NAC), nicotinic acid (NA) and MTT were all purchased from Sigma-Aldrich. SbIII-resistant parasites were generated by a stepwise approach starting with a drug concentration corresponding to the EC_{50} for that strain. Growth curve and EC_{50} were determined starting from an inoculum of 10^6 parasites/mL in 5 mL of complete medium, unless otherwise stated. Parasite density was determined daily (growth kinetics) or after 3 days of incubation with the drug (EC_{50} determination) using a flow cytometer[14] or by measuring the OD at 600 nm (for graphical convenience, OD values were multiplied by 1000). All EC_{50} values were obtained with GraphPad Prism v5 software using a sigmoidal dose-response model with variable slope. Cell viability assays on edited parasites were performed using a MTT test. In this assay, the yellow tetrazolium MTT dye was reduced to insoluble formazan crystals (purple color) in living cells using NADH as reducing agent. Briefly, 100µl of parasite cultures were mixed with 10µL of a MTT solution (10 mg/mL in PBS) and incubated 4h at 26°C. The reaction was stopped with 100 µL of lysis solution (50% isopropanol/10% SDS) and the plates were incubated for an additional 30 min with gentle shaking in the dark. The change in colour from yellow to purple was read at an absorbance of 600 nm.

NAD(H)/NADP(H) quantification

Total (NAD+ plus NADH) or individual (NAD+ and NADH) dinucleotides were quantified using the bioluminescent NAD/NADH-Glo™ Assay (Promega) following manufacturer's instructions. This kit uses a proluciferin substrate to produce a light signal proportional to the amount of NAD and/or NADH present in the samples. Total (NADP+ plus NADPH) and individual (NADP+ and NADPH) phosphorylated forms were quantified similarly using the NADP/NADPH-Glo™

Assay kit (Promega). Data are expressed as the mean value (±SD) of Relative Luminescence Units (RLU) obtained for 10^6 parasites and after 60 min of incubation.

Quantitative RT-PCR analyses (qRT-PCR)

All primers used in this study were designed with the primer3Plus software and are listed in table S1. Total RNA was extracted from parasite cultures in the exponential phase of growth using the RNeasy+ Mini Kit (Qiagen) with an additional treatment with turbo DNA-free DNase (Thermo Fischer Scientific). Two µg of total RNA was transcribed into complementary DNA (cDNA) using the Superscript reverse transcriptase III (Invitrogen) and oligo(dT)12-18 primers (Thermo Fischer Scientific), according to the manufacturer's instructions. Diluted cDNA (1/10) was used for the qPCR reactions in 10 µL final volume with SYBR Green I Master on a LightCycler480 (Roche). The relative expression of each gene was determined from two biological replicates with the $2^{-\Delta\Delta CT}$ method and the *GAPDH* gene as reference, using the LightCycler480 software.

CRISPR/Cas9 genome editing and off-target mutation analysis

The marker-free nucleotide editing approach developed in *P. Falciparum*[18] was adapted to introduce the H451Y mutation in the *L. major* reference strain. The 20nt single guide RNA (sgRNA) sequence TTTGATCGACTCCGAGCACT (the targeted nucleotide is underlined) was based on the *LmjF.33.1710* orthologue gene sequence. Plasmids were constructed as described in[17]. Briefly, a donor DNA sequence that consists of an 880 bp-long intragenic region of *LmjF.33.1710* gene was generated by PCR fusion using the modified primer pairs Lm1F/Lm1R and Lm2F/Lm2R (Table S1) to create the C1351T mutation and a "shield" silent mutation (G1356T) in the protospacer adjacent motif (PAM) to prevent further Cas9-mediated cleavage (Figure 2f). The donor DNA sequence was cloned in the pLS5 plasmid digested with *Kpn*I and *Xba*I. To obtain the 20nt sgRNA sequence surrounded by the 15nt adaptors necessary for In-Fusion® cloning, the two oligonucleotides Seed_F and Seed_R were annealed by incubation in boiling water for 2min followed by gentle cooling in room-temperature water for 2h. The sgRNA sequence and adaptors were then cloned in the *Bsg*I-digested pLS5-donor DNA plasmid using the In-Fusion HD cloning kit (Clonetech). pLS5-donor DNA plasmids with and without the sgRNA sequence were transfected in the *L. major* Friedlin strain that harbours the pTCAS9 plasmid[17] to generate edited (Lm_H451Y) and control (Lm_ctrl) cell lines,

respectively. After transfection and selection with hygromycin and puromycin, gene edition was checked by PCR amplification and Sanger sequencing using the LmiSCAMK_F/LmiSCAMK_R primer pair (Table S1). Once heterozygosity was confirmed in the mutated locus, parasites were cloned by limiting dilution. A parasite clone containing the homozygous desired and shield mutations (named Lm_H451Y) was selected for subsequent phenotype analyses. To confirm the absence of off-target mutations, the genomes of Lm_ctrl and Lm_H451Y strains were sequenced (see below) and off-target candidates (up to five mismatches allowed) were identified using the Protospacer Workbench software suite[19]. For each candidate, the vicinity (within a 21nt window) to specific INDELs of the edited cell lines was assessed as described in Vasquez *et al.*[20] (Table S2).

WGS and analyses

Parasite genomic DNA was extracted using the QIAamp DNA Mini Kit (Qiagen). A paired-end sequencing library for Δ*pnc1* parasites was prepared with the Nextera DNA Sample Preparation Kit (Illumina) and sequenced on an Illumina HiSeq 2500 (2x250 bp) apparatus. DNA samples from the KO-SbR, Lm_ctrl, Lm_H451Y and Lm_H451Y-SbR strains were sheared using a Bioruptor Pico sonication device (Diagenode) to yield ≈400 bp fragments. Libraries were constructed for WGS as previously described[21]. Paired-end sequencing (2 x 150 bp) was performed on an Illumina MiSeq apparatus with the MiSeq Reagent Kit V2. The presence of SNPs and INDELs was determined using the EuPathDB Galaxy platform[22] and the workflow pipeline for "Variant Calling, paired-end sequencing" and pre-loaded reference genomes for the *L. infantum* JPCM5 and *L. major* Friedlin strains (TritrypDB build 29). Filtered Variant Call Format (VCF) files corresponding to SNPs and INDELs with an impact on coding sequences were compared between the Δ*pnc1* and KO-SbR libraries. Specific SNPs/INDELs detected in KO-SbR (16 SNPs and 15 INDELs) were manually verified with the IGV 2.4.8 visualization tool, and eliminated if already present in the Δ*pnc1* parental line. After this verification step, only three specific SNPs were retained for analysis (Table S3). The same strategy was used to compare SNPs/INDELs in the Lm_ctrl, Lm_H451Y and Lm_H451Y-SbR libraries and only SNPs and INDELS with read depth >2 were kept for further analysis (Table S4). The CNV-seq pipeline was used to identify CNVs potentially associated with drug resistance[23]. This pipeline identifies localized regions in which the read depth normalized across the length of the chromosome differs significantly between samples. For Δ*pnc1* and KO-SbR pairwise comparisons, a 3kb

window size was chosen, but similar results were obtained with smaller and larger window sizes (Table S5). For Lm_H451Y and Lm_H451Y-SbR pairwise comparisons, the sliding window size was automatically determined (4265 bp). Input hits files were derived from the Binary Alignment Map (BAM) files generated by the EupathDB Variant Calling pipeline.

Accession number

All sequencing data have been submitted to the European Nucleotide Archive (ENA) and are available under the accession number PRJEB27329.

Results

Δ*pnc1 parasites are highly susceptible to SbIII*

When grown in SDM79 medium, Δ*pnc1* promastigotes had similar growth rates than wild type (WT) parasites (Figure 1b). However, they are about ten-fold more susceptible to SbIII (EC_{50} Δ*pnc1* = 2. 51 µg/mL; EC_{50} WT = 20.92 µg/mL) (Figure 1c). This phenotype could be rescued by NA supplementation in the growth medium (Figure 1c). NA supplementation also induced a dose-dependent increase of both NAD(H) and NADP(H) content in Δ*pnc1* parasites where these pools are significantly depleted (Figure 1d). Conversely, it did not have any effect on NAD(H) and NADP(H) content in WT parasites (Figure 1d). Individual dinucleotides measurements showed that Δ*pnc1* parasites were specifically depleted in NAD+ and NADPH forms (Figure 1e). As the *Leishmania* redox homeostasis is also maintained by *de novo* biosynthesis of reduced trypanothione (Figure 1a), we tested whether supplementation with trypanothione precursors could restore the physiological SbIII susceptibility in Δ*pnc1* parasites. Supplementation with N-acetyl-cysteine (NAC) or reduced glutathione (GSH) decreased the susceptibility of Δ*pnc1* parasites to SbIII (Figure 1f). Altogether, these results established a direct connection between *Leishmania* NAD+ metabolism, SbIII toxicity and thiol metabolism (Figure 1a). qRT-PCR assays further indicated that known genes involved in SbIII mode of action and resistance were similarly transcribed in Δ*pnc1* and WT parasites, except for *GSH1*, the rate-limiting step in glutathione biosynthesis, for which the transcript level was increased 2-fold in Δ*pnc1* (Figure 1g).

Δ*pnc1 parasites resistant to SbIII show a single amino acid substitution in the SCAMK gene*

To better understand the link between NAD+ homeostasis and SbIII susceptibility, we tried to generate SbIII-resistant WT and Δ*pnc1* parasites (named WT-SbR and KO-SbR, respectively) by stepwise selection in the presence of increasing concentrations of the drug. We could select KO-SbR parasites that proliferated in the presence of up to 320 µg/mL of SbIII (EC_{50} = 309 µg/mL), but not at higher concentrations (Figure 2a). In WT-SbR parasites (EC_{50} >1000µg/mL), MRPA was ten-fold upregulated as compared with WT parasites (Figure 2b) which is in agreement with the known model of antimony resistance[3,4] and the presence of an extrachromosomal amplicon of 15 kb bearing *MRPA* gene in the WT-SbR strain (data not shown). Conversely, qRT-PCR analysis showed a modest, but paradoxical overexpression of

the genes encoding the AQP1 transporter and MRPA efflux-pump in KO-SbR parasites (Figure 2b). Moreover, the levels of NAD+, NADH, NADP+ and NADPH were similar in KO-SbR and Δ*pnc1* parasites (Figure 2c). As drug resistance in *Leishmania* is often associated with gene copy number variations (CNVs) or SNPs[24], we sequenced the genomes of Δ*pnc1* and KO-SbR parasites by Illumina paired-end sequencing. As expected, no read aligned to the *pnc1* gene, confirming its deletion in the both strains (Figure S1). All CNVs detected in KO-SbR mutants were located in non-coding telomeric or intergenic regions (Table S5). The look for non-synonymous SNPs only present in the KO-SbR strain identified a single homozygous mutation (C1351T) leading to the H451Y substitution in a putative protein kinase gene (*LinJ.33.1810*) (Table S3). The fixation of the H451Y mutation in KO-SbR parasites was confirmed by PCR and Sanger sequencing (Figure 2d). Interestingly, another point mutation (E629K) in the C-terminus of the *LinJ.33.1810* gene was already described in a *L. infantum* SbIII-resistant strain bearing *MRPA* amplification[25]. This single copy gene defines a new kinase family recently named SCAMK[26] that is specific to Metakinetoplastina protists and functionally related to the calcium-dependent protein kinases (CDPKs) present in plants and protozoans[27]. CDPKs have been widely studied in apicomplexan parasites where they are considered to be important signal transducers involved in parasite motility, invasion or host cell egress[28]. Specifically, Ca^{2+} binding to the EF-hand domains of CDPKs induces a global conformational change of the protein, resulting in the activation of the kinase activity. The H residue in position 451, which is mutated in the KO-SbR strain, is located within the calcium-binding site of the third EF-hand domain of *Leishmania* SCAMK, and is conserved across kinetoplastids (Figure 2e).

The H451Y mutation generates SbIII tolerant Leishmania parasites

To gain insight into the role of the H451Y mutation in SbIII resistance, we used the CRISPR/cas9 genome editing technology[17] with a marker-free nucleotide editing approach[18] to introduce the H451Y mutation in the *Leishmania major* WT "Friedlin" reference strain. *L. major* parasites expressing Cas9 from an episomal plasmid were transfected with a second plasmid bearing an sgRNA complementary to the *L. major SCAMK* orthologue (*LmjF.33.1710*), and a donor sequence including the desired mutation (C1351T) and a shield mutation (G1356T) in the PAM motif (Lm_H451Y strain) (Figure 2f). As a control, we transfected parasites with the same plasmid backbone, but without the sgRNA (Lm_ctrl strain) (Figure 2g). After selection and cloning, we confirmed the presence of the H451Y mutation (Figure 2g) and

the absence of off-target mutations (Table S2) by Sanger and WGS, respectively. Phenotype analyses indicated that Lm_ctrl and Lm_H451Y strains had similar growth rates (Figure 3a). The SbIII susceptibility of both strains was compared using a MTT-based assay test and an inoculum of 10^6 parasites/mL. As shown in figure 3b, Lm_H451Y parasites are not more resistant than controls. Surprisingly, Lm_H451Y (but not Lm_ctrl) parasites exposed to the highest drug concentrations resumed growth after seven days in culture (Figure 3c). Analysis of the growth curves obtained starting from a higher parasite inoculum (4.10^6 parasites/mL) and using cytocidal concentrations of SbIII showed that Lm_H451Y parasites can survive and slowly proliferate in the presence of 1000 µg/mL of SbIII, which is the limit of SbIII solubility in the culture medium (Figure 3d). In a parallel experiment, the viability of edited parasites exposed to maximal SbIII concentrations has been confirmed and quantified by MTT-based assays performed at days 3 and 5 of culture (Figure 3e). Light-microscopy examination after exposure to the maximal concentration of SbIII revealed the presence of a heterogenous population of dead and unstressed promastigote forms in Lm_H451Y cultures, and the absence of surviving parasites in Lm_ctrl cultures (Figures 3f and S2). In agreement, we detected intact high molecular weight genomic DNA in all tested conditions for Lm_H451Y parasites, but only up to 250 µg/mL of SbIII for Lm_ctrl parasites (Figure 3g). The ability of a microorganism to survive lethal concentrations of a drug while keeping similar EC_{50} than susceptible strains is characteristic of drug tolerant/persistent microorganisms[29]. This phenomenon is known to facilitate drug resistance acquisition in bacteria but remains largely understudied in protozoan parasites[30]. To confirm the role of the H451Y mutation in *Leishmania* SbIII tolerance, we transiently exposed parasites to various bolus doses of SbIII for two days, and followed their growth after drug withdrawal. The growth of Lm_ctrl parasites was delayed and they could survive after transient exposure to SbIII concentrations up to 400 µg/mL (Figure 3h). Conversely, Lm_H451Y parasites recovered within 10 days post-bolus, whatever the concentration of SbIII used (Figure 3h). The toxicity of most anti-leishmanial drugs has been partly attributed to induction of reactive oxygen species (ROS) formation and consequently to oxidative damage. Therefore, we carried out similar growth curve experiments in the presence of miltefosine, amphotericin B, the oxidative stress inducer menadione, or H_2O_2 (Figure S3). We did not detect any difference between Lm_H451Y and Lm_ctrl parasites in all tested conditions, suggesting that the tolerance phenotype induced by the H451Y mutation is specific to SbIII mode of action and does not involve a generic response

to oxidative stress. Next, we tested whether Lm_H451Y parasites were prone to rapidly develop resistance to SbIII. As expected, highly resistant Lm_H451Y parasites (named Lm_H451Y-SbR) were selected after only five passages (P5) in the presence of 1000 µg/mL of SbIII (EC_{50} >1000 µg/mL) and this resistance phenotype remained stable up to P15 (Figure 3i). Genome sequencing of Lm_H451Y-SbR parasites cultured for 10 passages in the presence of 1000 µg/mL of SbIII did not reveal any new CNV compared with the Lm_H451Y parental cell line. Moreover, non-synonymous SNPs specific to Lm_H451Y-SbR were all heterozygous and only concerned hypothetical proteins or factors not known to be involved in SbIII resistance (Table S4). These results corroborate our initial observations in the *L. infantum* KO-SbR mutant and show that the H451Y mutation is necessary and sufficient to generate SbIII-tolerant parasites that can rapidly evolve into resistant parasites in the presence of drug pressure.

Discussion

Drug resistance in eukaryotic microorganisms shares many similarities with antibiotic resistance in bacteria[3]. Our knowledge about drug resistance mechanisms in *Leishmania* (and other protozoan parasites) mainly results from experiments using growth inhibitory measurements that determine the lowest drug concentration needed to inhibits parasite growth by 50% (EC_{50}). Mechanisms of drug action and resistance patterns can be however different when measured at dosages that kill the parasite, not just inhibit its growth[31]. Moreover, these approaches do not allow the identification of parasite subpopulations with variable levels of resistance. In bacteria or fungi, drug tolerant subpopulations (also known as "persisters") can survive at lethal drug concentrations while being still sensitive to cytostatic effect of the drug. The mechanisms leading to persisters formation are diverse and can include genetic mutations that increase the proportion of persister cells within a population[32,33]. Importantly, persisters are known to cause treatment failure due to relapsing infections and behave as an evolutionary reservoir of drug resistance[30,34,35]. The phenomenon of drug tolerance/persistence in protozoan parasites and its link with parasite drug resistance and treatment failure have been poorly studied to date. In trypanosomatids, the ability of drug-sensitive parasites to survive a lethal and prolonged drug exposure has been recently described in *Trypanosoma cruzi*[36] and *Leishmania*[37]. However, these phenotypes have been attributed to clearly distinct mechanisms involving a metabolic dormancy state and a genetic preadaptation to resistance, respectively.

In this study, we report that (i) *Leishmania* NAD+ depletion led to SbIII hypersusceptibility that is rescued by NAD+ precursor or trypanothione precursors supplementation; (ii) NAD+ depleted parasites can develop SbIII resistance through a single amino acid substitution in a metakinetoplastid-specific kinase; (iii) this mutation makes *Leishmania* parasites tolerant to high concentrations of SbIII and facilitates the emergence of resistant parasites without additional genomic modification. Although these findings have been obtained in mutants selected under laboratory conditions *in vitro*, they provide novel insights into the mode of action of antimony and establish that the orphan *Leishmania* kinase SCAMK is a new central actor of SbIII mode of action and resistance. Because the H451Y mutation is precisely located within the calcium-binding site of the third EF-hand domain of *Leishmania* SCAMK, we can speculate that it should directly impair Ca^{2+} binding and the associated conformational change

required for the enzymatic activation of CDPKs. The study of the structural consequences of the H451Y mutation should help us in understanding how this orphan kinase integrates calcium signaling to control the lethal effect of SbIII and could result in new therapeutic applications. We were unable to analyse the tolerance phenotype of edited parasites in the intracellular amastigote stage because the *L. major* strain used in this study is a reference strain that lost its virulence due to repeated passages *in vitro*. Further work is therefore required to determine whether this mutation can lead to treatment failure and persistent infection *in vivo* and to assess whether it is harmful or whether it can be spread in natural populations. Nevertheless, the correlation between *Leishmania SCAMK* gene polymorphisms and antimony treatment failure in clinical isolates could constitute the first step towards the identification of a new molecular marker of antimony tolerance/resistance in the field.

Acknowledgements: We thank the MGX platform (Montpellier, France) and Dr Mallorie Hide for HiSeq sequencing, and the UMR DIADE (Dynadiv team) for library preparation and MiSeq sequencing at CIRAD (Montpellier, France). We are also thankful to Elisabetta Andermarcher for assistance in editing the manuscript.

Funding: This work was supported by the Institut de Recherche pour le Développement (IRD), the Centre National de la Recherche Scientifique (CNRS), the French Ministry of Research and the Centre Hospitalier Universitaire of Montpellier institutional fundings. LS, JJLR, and YS were supported by the Laboratoire d'Excellence (LabEx) ParaFrap (the French Parasitology Alliance for Health Care, grant number ANR-11- LABX-0024).

References

1. Burza S, Croft SL, Boelaert M. Leishmaniasis. *The Lancet* 2018; **392**: 951–70.

2. Wyllie S. Dual action of antimonial drugs on thiol redox metabolism in the human pathogen *Leishmania donovani*. *J Biol Chem* 2004; **279**: 39925–32.

3. Fairlamb AH, Gow NAR, Matthews KR *et al.* Drug resistance in eukaryotic microorganisms. *Nat Microbiol* 2016; **1**: 16092.

4. Ponte-Sucre A, Gamarro F, Dujardin J-C *et al.* Drug resistance and treatment failure in leishmaniasis: A 21st century challenge. *PLoS Negl Trop Dis* 2017; **11**: e0006052–24.

5. Leprohon P, Légaré D, Ouellette M. Intracellular localization of the ABCC proteins of *Leishmania* and their role in resistance to antimonials. *Antimicrob Agents Chemother* 2009; **53**: 2646–9.

6. Arcari T, Manzano JI, Gamarro F. ABCI3 is a new mitochondrial ABC transporter from *Leishmania major* involved in susceptibility to antimonials and infectivity. *Antimicrob Agents Chemother* 2017; **61**: 113–8.

7. Manzano JI, Garcia-Hernandez R, Castanys S *et al.* A new ABC half-transporter in *Leishmania major* is involved in resistance to antimony. *Antimicrob Agents Chemother* 2013; **57**: 3719–30.

8. Perea A, Manzano JI, Castanys S *et al.* The LABCG2 transporter from the protozoan parasite *Leishmania* is involved in antimony resistance. *Antimicrob Agents Chemother* 2016; **60**: 3489–96.

9. Tejera Nevado P, Bifeld E, Höhn K *et al*. A telomeric cluster of antimony resistance genes on chromosome 34 of *Leishmania infantum*. *Antimicrob Agents Chemother* 2016; **60**: 5262–75.

10. Vergnes B, Gourbal B, Girard I *et al.* A proteomics screen implicates HSP83 and a small kinetoplastid calpain-related protein in drug resistance in *Leishmania donovani* clinical field isolates by modulating drug-induced programmed cell death. *Mol Cell Proteomics* 2007; **6**: 88–101.

11. Garg M, Goyal N. MAPK1 of *Leishmania donovani* modulates antimony susceptibility by downregulating P-glycoprotein efflux pumps. *Antimicrob Agents Chemother* 2015; **59**: 3853–63.

12. Gazanion E, Fernandez-Prada C, Papadopoulou B *et al*. Cos-Seq for high-throughput identification of drug target and resistance mechanisms in the protozoan parasite *Leishmania*. *Proc Natl Acad Sci USA* 2016; **113**: E3012–21.

13. Choudhury K, Zander D, Kube M *et al.* Identification of a *Leishmania infantum* gene mediating resistance to miltefosine and SbIII. *Int J Parasitol* 2008; **38**: 1411–23.

14. Gazanion E, Garcia D, Silvestre R *et al.* The *Leishmania* nicotinamidase is essential for NAD(+) production and parasite proliferation. *Mol Microbiol* 2011; **82**: 21–38.

15. Michels PAM, Avilán L. The NAD(+) metabolism of *Leishmania*, notably the enzyme nicotinamidase involved in NAD(+) salvage, offers prospects for development of anti-parasite chemotherapy. *Mol Microbiol* 2011; **82**: 4–8.

16. Mesquita I, Varela P, Belinha A *et al.* Exploring NAD(+) metabolism in host-pathogen interactions. *Cell Mol Life Sci* 2016; **73**: 1225–36.

17. Sollelis L, Ghorbal M, MacPherson CR *et al.* First efficient CRISPR-Cas9-mediated genome editing in *Leishmania* parasites. *Cell Microbiol* 2015; **17**: 1405–12.

18. Ghorbal M, Gorman M, MacPherson CR *et al*. Genome editing in the human malaria parasite *Plasmodium falciparum* using the CRISPR-Cas9 system. *Nat Biotechnol* 2014; **32**: 819–21.

19. MacPherson CR, Scherf A. Flexible guide-RNA design for CRISPR applications using Protospacer Workbench. *Nat Biotechnol* 2015; **33**: 805–6.

20. Vasquez JJ, Wedel C, Cosentino RO *et al.* Exploiting CRISPR-Cas9 technology to investigate individual histone modifications. *Nucleic Acids Res* 2018; **46**: e106.

21. Mariac C, Scarcelli N, Pouzadou J *et al.* Cost-effective enrichment hybridization capture of chloroplast genomes at deep multiplexing levels for population genetics and phylogeography studies. *Mol Ecol Resour* 2014; **14**: 1103–13.

22. Aurrecoechea C, Barreto A, Basenko EY *et al.* EuPathDB: the eukaryotic pathogen genomics database resource. *Nucleic Acids Res* 2017; **45**: D581–91.

23. Xie C, Tammi MT. CNV-seq, a new method to detect copy number variation using high-throughput sequencing. *BMC Bioinformatics* 2009; **10**: 80–9.

24. Leprohon P, Fernandez-Prada C, Gazanion E *et al.* Drug resistance analysis by next generation sequencing in *Leishmania*. *Int J Parasitol Drugs Drug Resist* 2015; **5**: 26–35.

25. Brotherton MC, Bourassa S, Leprohon P *et al.* Proteomic and genomic analyses of antimony resistant *Leishmania infantum* mutant. *PLoS ONE* 2013; **8**: e81899.

26. Chen F, Zhang L, Lin Z *et al.* Identification of a novel fused gene family implicates convergent evolution in eukaryotic calcium signaling. *BMC Genomics* 2018; **19**: 306.

27. Harper JF, Harmon A. Plants, symbiosis and parasites: a calcium signalling connection. *Nat Rev Mol Cell Biol* 2005; **6**: 555–66.

28. Billker O, Lourido S, Sibley LD. Calcium-dependent signaling and kinases in apicomplexan parasites. *Cell Host Microbe* 2009; **5**: 612–22.

29. Fisher RA, Gollan B, Helaine S. Persistent bacterial infections and persister cells. *Nat Rev Microbiol* 2017; **15**: 453–64.

30. Cohen NR, Lobritz MA, Collins JJ. Microbial persistence and the road to drug resistance. *Cell Host Microbe* 2013; **13**: 632–42.

31. Roepe PD. To kill or not to kill, that is the question: cytocidal antimalarial drug resistance. *Trends Parasitol* 2014; **30**: 130–5.

32. Michiels JE, Van den Bergh B, Verstraeten N *et al.* Molecular mechanisms and clinical implications of bacterial persistence. *Drug Resist Updat* 2016; **29**: 76–89.

33. Balaban NQ, Helaine S, Lewis K *et al.* Definitions and guidelines for research on antibiotic persistence. *Nat Rev Microbiol* 2019; doi: 10.1038/s41579-019-0196-3. [Epub ahead of print]

34. Delarze E, Sanglard D. Defining the frontiers between antifungal resistance, tolerance and the concept of persistence. *Drug Resist Updat* 2015; **23**: 12–9.

35. Levin-Reisman I, Ronin I, Gefen O *et al.* Antibiotic tolerance facilitates the evolution of resistance. *Science* 2017; **355**: 826–30.

36. Sánchez-Valdéz FJ, Padilla A, Wang W *et al.* Spontaneous dormancy protects *Trypanosoma cruzi* during extended drug exposure. *eLife* 2018; **7**: 833.

37. Dumetz F, Cuypers B, Imamura H *et al.* Molecular preadaptation to antimony resistance in *Leishmania donovani* on the Indian subcontinent. *mSphere* 2018; **3**: e00548–17.

Figure legends

Figure 1. Δ*pnc1* parasites are highly susceptible to SbIII. (a) Schematic representation of the cross-talk between *Leishmania* NAD+ metabolism, trivalent antimony (SbIII) mode of action and thiol metabolism. NA, nicotinic acid; NAm, nicotinamide; NR, nicotinamide riboside; NAMN, nicotinic acid mononucleotide; NAAD, nicotinic acid dinucleotide; NADK, NAD+ kinase; PPP, pentose phosphate pathway; G6PDH, glucose-6-phosphate dehydrogenase; AQP1, aquaglyceroporin 1; TR, trypanothione reductase; T(SH)2, reduced trypanothione; T(S)2, oxidized trypanothione; TXN1, tryparedoxin 1; MRPA, ABCC3 transporter; Glu, glutamate; Cys, cysteine; Orn, ornithine; GSH1, gamma-glutamylcysteine synthetase; GSH, glutathione; Spd, spermidine; GSpdS, glutathionylspermidine synthetase; Gspd, glutathionylspermidine; TryS, trypanothione synthase. **(b)** Growth curves of *L. infantum* WT and Δ*pnc1* promastigotes in SDM79 medium supplemented with NA (1, 10 and 100 µM). Data are representative of three independent experiments. **(c)** Effect of SbIII on the growth kinetics of *L. infantum* WT and Δ*pnc1* parasites (supplemented or not with 1, 10 and 100 µM NA). Data are the mean ± SD of two biological replicates and are representative of at least five independent experiments. **(d)** Intracellular NAD(H) (left) and NADP(H) (right) levels measured in *L. infantum* WT (black bars) and Δ*pnc1* (white bars) parasites after 2 days of culture in the presence of increasing concentrations of NA (quantification of parallel series of cultures as described in Methods section). Values are expressed as Relative Luminescence Units (RLU) for 10^6 parasites and are the mean ± SD of triplicate measurements. **(e)** Relative quantification of NAD+, NADH, NADP+ and NADPH in WT and Δ*pnc1* parasites after 2 days of growth. Data are the mean ± SD of duplicate measurements and are representative of two independent experiments. **(f)** Effect of GSH and N-acetyl cysteine (NAC) supplementation on the growth kinetics of *L. infantum* WT and Δ*pnc1* parasites in the presence of increasing concentrations of SbIII. Data are the mean ± SD of duplicate measurements and are representative of three independent experiments. **(g)** Relative gene expression levels of candidate genes involved in SbIII mode of action/resistance in Δ*pnc1* parasites relative to the WT strain (see above for abbreviations). The fold-change cut-offs (0.5 and 1.5) are represented by dashed lines.

Figure 2. SbIII-resistant Δ*pnc1* parasites show a single amino acid substitution (H451Y) in *SCAMK* gene. (a) SbIII susceptibility of *L. infantum* WT-SbR and KO-SbR parasites. Growth in

the presence of increasing concentrations of SbIII was monitored at 72h by measuring the culture OD at 600 nm. Data are the mean ± SD of duplicate measurements and are representative of three independent experiments. **(b)** Relative quantification of transcript abundance in WT-SbR relative to WT parasites (left panel) and in KO-SbR relative to Δ*pnc1* parasites (right panel). The fold-change cut-offs (0.5 and 1.5) are represented by dashed lines. **(c)** Quantification of NAD+, NADH, NADP+ and NADPH levels in KO-SbR parasites relative to Δ*pnc1* parental line after 2 days of growth. Dotted line, ratio = 1. Data are the mean ± SD RLU ratio values obtained from two biological replicates, each measured in duplicate. **(d)** Comparison of the *LinJ.33.1810* gene sequences in Δ*pnc1* (top) and KO-SbR (bottom) parasites showing the C to T substitution (asterisk) in KO-SbR parasites. **(e)** Schematic representation of the functional domains present in the protein encoded by the *LinJ.33.1810* gene using the ScanProsite tool (https://prosite.expasy.org/scanprosite/). Lower panel: alignment of the EF-hand domain 3 from *LinJ.33.1810* orthologues in *L. major* (*LmjF.33.1710*), *L. donovani* (*LdBPK_331810.1*), *L. braziliensis* (*LbrM.33.1980*), *Trypanosoma brucei* (*Tb927.2.1820*) and *Trypanosoma cruzi* (*TcCLB.510257.130*). The black arrow indicates the conserved H residue in position 451. The calcium-binding site of EF hand 3 (EF-loop 3) is underlined. **(f)** Position of the sgRNA sequence and the protospacer adjacent motif (PAM) in the *LmjF.33.1710* sequence used to introduce the H451Y mutation in *L. major* with the CRISPR/Cas9 gene editing system. The partial donor DNA sequence illustrates the presence of the targeted and shield mutations. **(g)** Left: schematic representation of the plasmids used to generate the Lm_ctrl and Lm_H451Y strains. Right: chromatograms corresponding to part of the *LmjF.33.1710* gene sequence (Sanger method). The targeted and shield mutations are indicated by a red and a green asterisk, respectively.

Figure 3. The H451Y mutation generates SbIII tolerant and resistant *Leishmania* parasites. **(a)** Growth curves of Lm_ctrl and Lm_H451Y parasites in SDM79 medium. Data are the mean ± SD of two biological replicates and are representative of at least three independent experiments. **(b)** SbIII susceptibility of Lm_ctrl and Lm_H451Y parasites. Growth in the presence of increasing concentrations of SbIII (25, 50, 100, 200, 400, 600 µg/mL) was monitored at 72h by MTT-based assay. Data are the mean ± SD of two biological replicates and representative of two independent experiments. **(c)** Same growth curves experiments as in (b) showing that Lm_H451Y parasites exposed to the highest SbIII concentrations restart to

growth after 7 days. **(d)** Growth curves of Lm-ctrl (left) and Lm_H451Y (right) parasites seeded at 4.10^6 parasites/mL and exposed to cytocidal concentrations of SbIII (250, 500 and 1000 µg/mL) for eight days. Data are the mean ± SD of duplicate OD measurements and are representative of three independent experiments. **(e)** Quantification of Lm_ctrl and Lm_H451Y parasites viability using MTT-based assays. Parasites were seeded at 4.10^6 parasites/mL and exposed to high concentrations of SbIII (100, 250, 500, 1000 µg/ml) for 3 and 5 days. Data are expressed as OD 600 nm values and are the mean ± SD of two biological replicates. **(f)** Light-microscopy images of Lm_ctrl (top panel) and Lm_H451Y (bottom panel) parasites exposed to 1000 µg/mL of SbIII for 3 days (EVOS FL inverted microscope and x20 magnification). **(g)** Integrity of genomic DNA extracted from 5 mL of parasite cultures seeded at 4.10^6 parasites/mL after 3 days of culture in the presence of different SbIII concentrations (0, 250, 500 and 1000 µg/mL). MW: GeneRuler 1kb DNA ladder. **(h)** Lm_ctrl (left) and Lm_H451Y (right) parasites were incubated with increasing concentrations of SbIII (100 to 800 µg/mL) for 48h. Parasites were then centrifuged, washed three times with PBS and grown in drug-free medium for ten days. The experiment timeline is shown at the bottom. Parasite density (OD) was checked daily. Data are the mean ± SD of two duplicate measurements and are representative of two independent experiments. **(i)** Growth inhibition assay of Lm_H451Y parasites cultured with 1000 µg/mL SbIII for 1 (P1), 5 (P5), 10 (P10) and 15 (P15) consecutive passages.

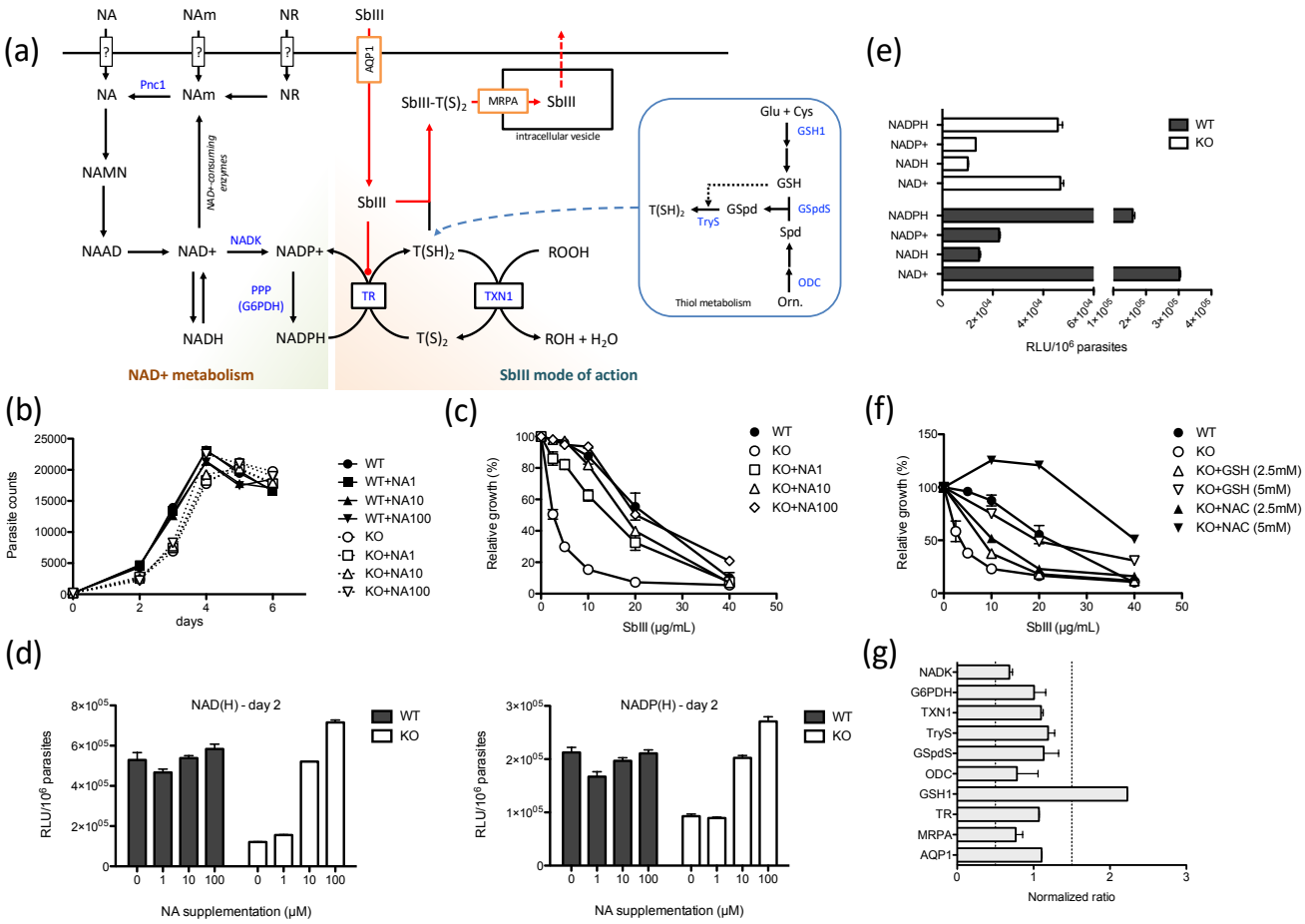
(a)
NA
NAm
NR
SbIII
AQP1
Pnc1
SbIII-T(S)2
MRPA
intracellular vesicle
NAMN
NAD+-consuming enzymes
NAAD
NAD+
NADK
NADP+
PPP (G6PDH)
NADH
NADPH
TR
T(SH)2
TXN1
ROOH
T(S)2
ROH + H2O
NAD+ metabolism
SbIII mode of action
Glu + Cys
GSH1
GSH
GSpd
GSpdS
Spd
TryS
ODC
Orn.
Thiol metabolism
(e)
WT
KO
RLU/10^6 parasites
(b)
Parasite counts
days
WT
WT+NA1
WT+NA10
WT+NA100
KO
KO+NA1
KO+NA10
KO+NA100
(c)
Relative growth (%)
SbIII (µg/mL)
(f)
KO+GSH (2.5mM)
KO+GSH (5mM)
KO+NAC (2.5mM)
KO+NAC (5mM)
(d)
NAD(H) - day 2
NADP(H) - day 2
RLU/10^6 parasites
NA supplementation (µM)
(g)
NADK
G6PDH
TXN1
TryS
GSpdS
ODC
GSH1
TR
MRPA
AQP1
Normalized ratio

Figure 1

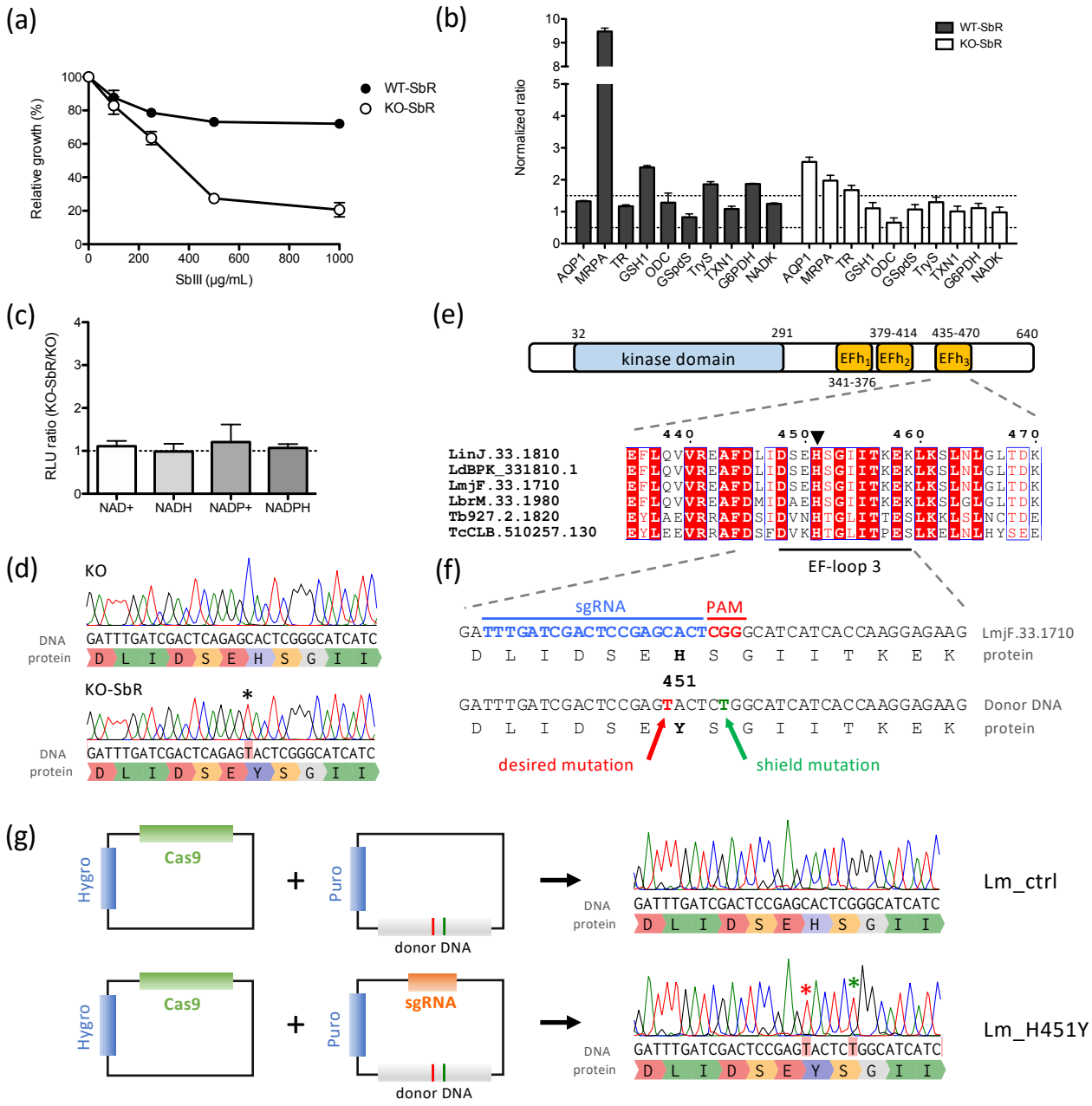
(a)
Relative growth (%)
SbIII (μg/mL)
WT-SbR
KO-SbR
(b)
Normalized ratio
WT-SbR
KO-SbR
AQP1
MRPA
TR
GSH1
ODC
GSpdS
TryS
TXN1
G6PDH
NADK
(c)
RLU ratio (KO-SbR/KO)
NAD+
NADH
NADP+
NADPH
(e)
kinase domain
EFh1
EFh2
EFh3
341-376
EF-loop 3
LinJ.33.1810
LdBPK_331810.1
LmjF.33.1710
LbrM.33.1980
Tb927.2.1820
TcCLB.510257.130
(d)
KO
KO-SbR
DNA
protein
(f)
sgRNA
PAM
LmjF.33.1710
Donor DNA
desired mutation
shield mutation
(g)
Hygro
Cas9
Puro
donor DNA
sgRNA
Lm_ctrl
Lm_H451Y

Figure 2

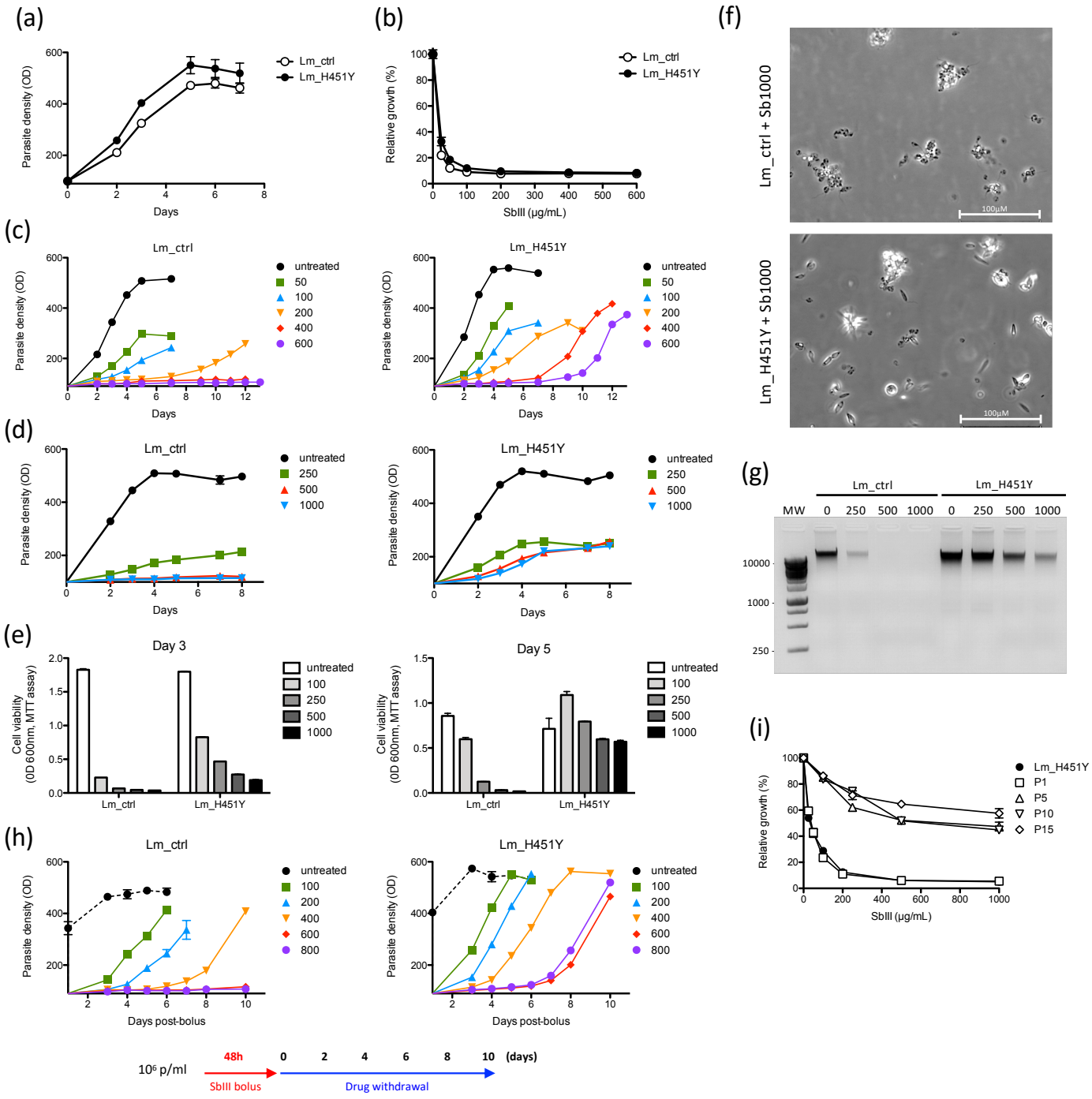
(a)
Parasite density (OD)
Days
Lm_ctrl
Lm_H451Y
(b)
Relative growth (%)
SbIII (µg/mL)
(c)
Lm_ctrl
Lm_H451Y
untreated
50
100
200
400
600
(d)
untreated
250
500
1000
(e)
Day 3
Day 5
Cell viability (OD 600nm, MTT assay)
(f)
Lm_ctrl + Sb1000
Lm_H451Y + Sb1000
100µM
(g)
MW
0
250
500
1000
10000
1000
250
(h)
untreated
100
200
400
600
800
Days post-bolus
10⁶ p/ml
48h
SbIII bolus
Drug withdrawal
(days)
(i)
P1
P5
P10
P15

Figure 3

Supplementary data

A single amino acid substitution (H451Y) in *Leishmania* calcium-dependent kinase SCAMK confers high tolerance and resistance to antimony. B Vergnes, E Gazanion, C Mariac, M Du Manoir, L Sollelis, JJ Lopez-Rubio, Y Sterkers, AL Bañuls.

Table S1. Primers used in this study.

Primer name	Sequence (5'-3')
Crispr/Cas9	
Lm_1F	CTGGTACCCATCACCCCTCAGATGAGC (KpnI)
Lm_1R	GATGATGCCAGAGTACTCGG
Lm_2F	CCGAGTACTCTGGCATCATC
Lm_2R	GCTCTAGAGTCGAGAAACCACTTGTGG (XbaI)
seed_F	CAGGCACCGCTGGTGGtttgatcgactccgagcactGTTTTAGAGCTAGAAAT
seed_R	ATTTCTAGCTCTAAAACagtgctcggagtcgatcaaaCCACCAGCGGTGCCTG
LmiSCAMK_F	CAACAGCCATCTCACCGTGC
LmiSCAMK_R	GGACAACGGGGTTTCACGTG
qRT-PCR	
gapdh_F	GACACGTCGATCCAGGAGAT
gapdh_R	AGCCCCACTCGTTGTCATAC
GSH1_F	ACTCCCGTACAATGCAGGAC
GSH1_R	GTAGCAGGGGTGAAGAGCTG
ODC_F	CGTCGACCTCTTCTTCCTTG
ODC_R	TCTCGATCGCACTCTTGTTG
TR_F	TGAACAGCATCAACGAGAGC
TR_R	TTGCTCGTGATGCAGAACTC
G6PDH_F	TGCAGATCACGTTCAAGGAG
G6PDH_R	CGGCTCAATGCACTTCAGTA
NADK_F	GATCAGGAAGACCAGGTGGA
NADK_R	ACAACTTGTGCTGCAAATCG
GspdS_F	AGTCCGACGCTCTCTGACAT
GspdS_R	GGAGACGTAGTGGTGGGAGA
TRYS_F	AGCCGATGTGGAAAGTCATC
TRYS_R	CCCATAGTTGCCACCAGACT
TXN1_F	TTGAAGCTGCAGAAGCAGAA
TXN1_R	GAAGTCCTCCTCCTCCTCGT
MRPA_F	GGACGTGGAAGAGAGAGTCG
MRPA_R	GTACTCGCCCATCAGAGAGC
AQP1-F	GAACTTCACGTCGCAGAACA
AQP1-R	GATGGCCATGTAGCTGGAGT

Table S2. Off-target mutation analysis. List of the off-target candidates identified with the Protospacer Workbench software (with RazerS 3, and five mismatches allowed).

#Target: TTTGATCGACTCCGAGCACT(CGG)
#Chromosome: LmjF.33
#Position: 795935
#Strand: +
#Doench-Root Activity: 0.177750

target
NGG PAM
non-canonical PAM

chromosome	position	strand	sequence	pam	mismatches	dra	score	< 20bp from a specific INDEL in Lm_H451Y
LmjF.33	795935	+	TTTGATCGACTCCGAGCACT	CGG	0	0.17774975685470332	1.0	
LmjF.25	827829	-	CTTGATTGACGCAGAGCACT	TGG	4	0.048381370162212375	0.0022051146716772154	NO
LmjF.31	1158568	-	TTGGATCGACTCAGGGCAGT	AGG	4	0.05825528097973003	0.0005192731021153846	NO
LmjF.30	1324740	-	TGTGAACGACTCCGGGCTCT	GAG	4	0.0	0.000512281696832579	NO
LmjF.36	706422	+	CTTGAGCGACTCAGAGTAGT	AGG	5	0.3237375902104075	0.00028025959499999994	NO
LmjF.16	692860	-	TTTCATCGGCTCCGCGCCCA	AAG	5	0.0	0.00012875219199189871	NO
LmjF.04	358636	+	TTTCAGCGACGCTGAGCACG	AAG	5	0.0	0.0005212929826708861	NO
LmjF.19	612710	+	TTTCTTCGAATCCGACAACT	TAG	5	0.0	0.000565260380487805	NO
LmjF.36	1305474	-	CTTCATCGACTACATGCACT	GGG	5	0.1253521096282401	0.00018433794370370374	NO
LmjF.35	576833	+	TTTGATCGCCTGGGAGCAGG	AGG	5	0.17388963529208032	0.00013826052225180001	NO
LmjF.27	942224	+	ATTGAGCGCCGCCGTGCACT	CGG	5	0.15677322326935583	0.0005158850416296295	NO
LmjF.33	796031	+	TTCGATGGACACGGAGCACA	AGG	5	0.04419561195415686	0.0005877012458031232	NO
LmjF.34	950998	+	GTTGCGCGACTCCGAGTGCT	CGG	5	0.2699483343642831	0.00044482702564102556	NO
LmjF.18	722184	-	TTTATTCGACTCAGAGCGCA	CGG	5	0.6556028597619067	0.0003042913397468355	NO
LmjF.30	370497	-	GCAGAACGACTGCGAGCACT	AGG	5	0.21520147439812617	0.002655410685714286	NO
LmjF.36	2457360	+	TTGCAACGACACCGAGCACG	CAG	5	0.0	0.0013451797386923078	NO
LmjF.36	1570009	-	TTTGGTCTGCTCCGAGCCCG	GGG	5	0.34862116391658615	0.0004744133939999999	NO
LmjF.18	575242	+	TTTCATCCACGCCGTGCACG	TGG	5	0.32245220558738613	0.0005966921620253165	NO
LmjF.27	636627	-	TTTGTTCGACTCAGGGCGAT	CAG	5	0.0	6.0081526399999974e-05	NO
LmjF.25	411227	-	TATGATCGACTCCGTTCATG	TAG	5	0.0	5.976304494545457e-05	NO
LmjF.08	529243	+	TTTGATCCTCTCCGAGAGCA	GAG	5	0.0	0.00017604737994216869	NO

Table S3. Heterozygous and homozygous non-synonymous SNPs identified in the coding sequences of KO-SbR mutants but not in the Δ*pnc1* parental line.

#CHROM	POS	GENE ID	PRODUCT DESCRIPTION	REF	ALT	AA change	QUAL	GT	DP	RO	AO
LinJ.33	689935	LinJ.33.1810	protein kinase	C	T	H451Y	376,64	1/1	12	0	12
LinJ.29	279621	LinJ.29.0790	heat shock protein 90 (LPG3)	G	A	R592C	293	0/1	18	6	12
LinJ.15	428514	LinJ.15.1070	glutamate dehydrogenase	G	C	Q917E	264,17	0/1	24	12	12

GT=Genotype, DP=Read Depth, RO=Reference allele observation count, AO=Alternate allele observation count

Table S4. Non-synonymous SNPs identified in the coding sequences of Lm_H451Y-SbR mutants, but not in Lm_ctrl and Lm_H451Y parasites.

#CHROM	POS	GENE ID	PRODUCT DESCRIPTION	REF	ALT	AA change	QUAL	GT	DP	RO	AO
LmjF.17	584469	LmjF.17.1200	hypothetical protein	C	T	A75V	61,93	0/1	10	6	4
LmjF.05	19975	LmjF.05.0060	major vault protein	T	A	S647T	61,93	0/1	10	6	4
LmjF.20	352500	LmjF.20.0850	pseudouridine synthase TruD	A	G	E288G	60,29	0/1	10	5	5
LmjF.34	1103815	LmjF.34.2480	hypothetical protein	G	A	stop	55,44	0/1	4	1	3
LmjF.30	915322	LmjF.30.2380	hypothetical protein	A	G	V255A	53,61	0/1	11	7	4

GT=Genotype, DP=Read Depth, RO=Reference allele observation count, AO=Alternate allele observation count

Table S5. Results of the CNV-seq method used to compare CNVs in SbIII-sensitive (KO) and SbIII-resistant (KO-SbR) Δ*pnc1* parasites.

CNV	#CHROM	START	END	SIZE (bp)	log2	p.value	COMMENT
CNVR_1	16	751	9750	9000	-1.362885	1.155912e-231	nc tel
CNVR_2	04	116251	122250	6000	0.7291408	8.793945e-86	nc tel
CNVR_3	04	467251	476250	9000	-1.065832	8.215468e-111	nc tel
CNVR_4	11	751	6750	6000	-1.67662	1.353293e-199	nc tel
CNVR_5	17	662251	668250	6000	-1.155018	9.593298e-88	nc tel
CNVR_6	24	863251	869250	6000	-0.8339029	7.110614e-53	nc tel
CNVR_7	32	751	6750	6000	-1.397065	8.888547e-158	nc tel
CNVR_8	35	219751	225750	6000	-0.8113096	4.357229e-54	part of LinJ.35.0530 (ppg5)
CNVR_9	18	716251	722250	6000	-1.402387	1.036969e-108	nc tel
CNVR_10	22	653251	660750	7500	-1.008428	2.584667e-92	nc tel
CNVR_11	02	326251	335250	9000	-0.7970366	1.0524e-81	nc tel
CNVR_12	12	751	8250	7500	-1.738381	0	nc tel
CNVR_13	23	751	6750	6000	-1.995511	0	nc tel
CNVR_14	30	1358251	1367250	9000	-1.276207	4.045936e-143	nc tel
CNVR_15	26	1046251	1052250	6000	-0.8611537	1.727647e-56	nc tel
CNVR_16	13	543751	549750	6000	-1.736291	4.360188e-204	nc inter

nc tel: non-coding telomeric extremity ; nc inter: non-coding intergenic sequence ; ppg5: member of the large and conserved family of proteophosphoglycan.

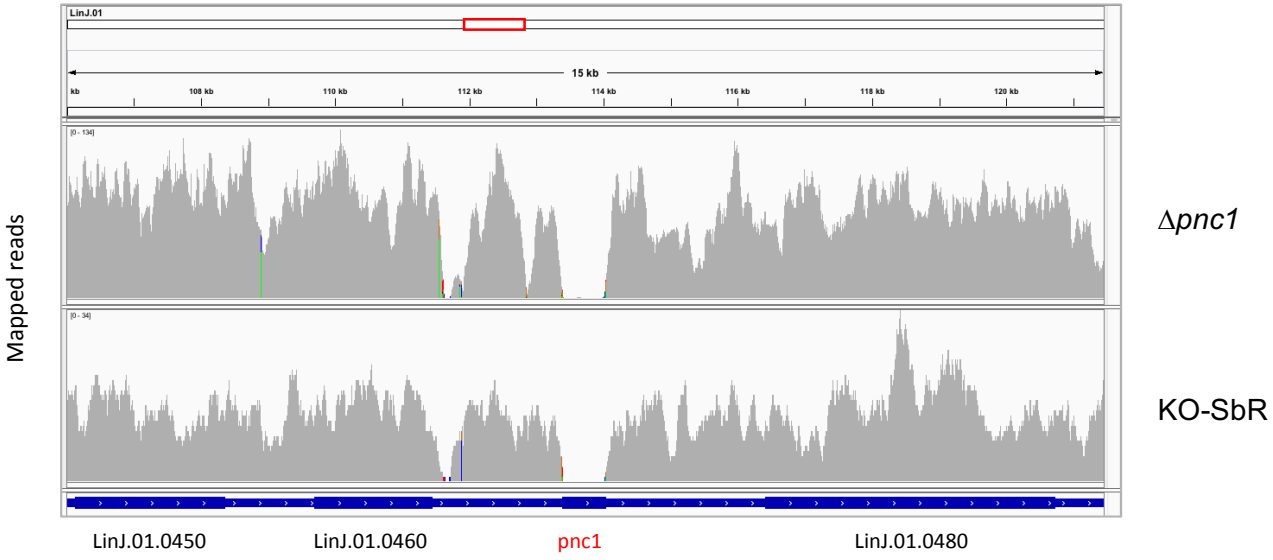

Figure S1. Validation of *pnc1* gene inactivation in sequenced strains. Read coverage (bam files) along chromosome 1 in the Δ*pnc1* and KO-SbR strains showing the lack of aligned reads for the *LinJ.01.0470* gene (*pnc1*).

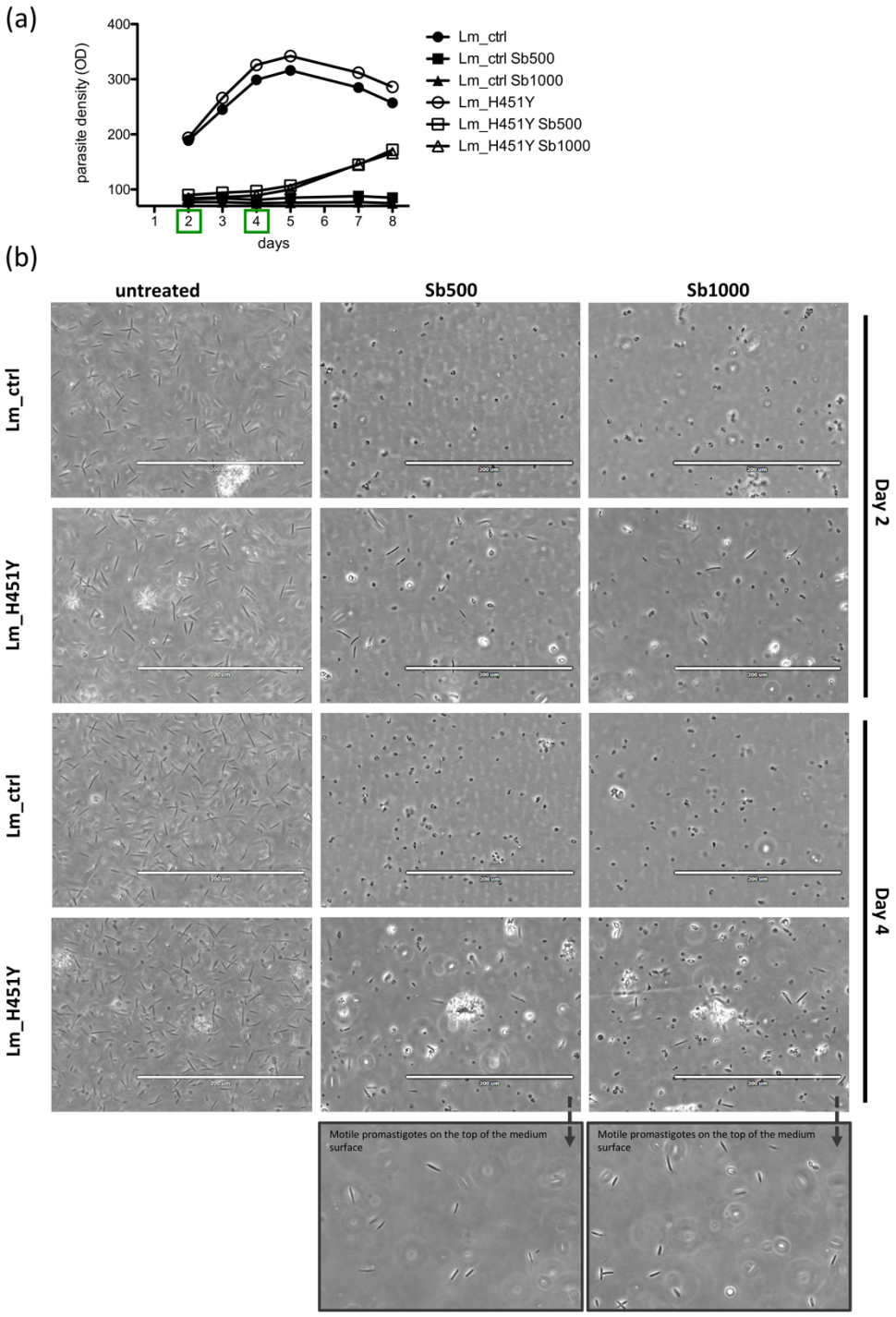

Figure S2. Action of cytocidal concentrations of SbIII on control and edited parasite populations. (a) Follow-up of parasite density in control (Lm_ctrl) and edited (Lm_H451Y) populations seeded at 4.10^6 parasites/mL and exposed to cytocidal concentrations of SbIII (500 and 1000 µg/mL). (b) Images of the parasite cultures described in (a) taken after 2 and 4 days of growth (EVOS FL inverted microscope with x20 magnification).

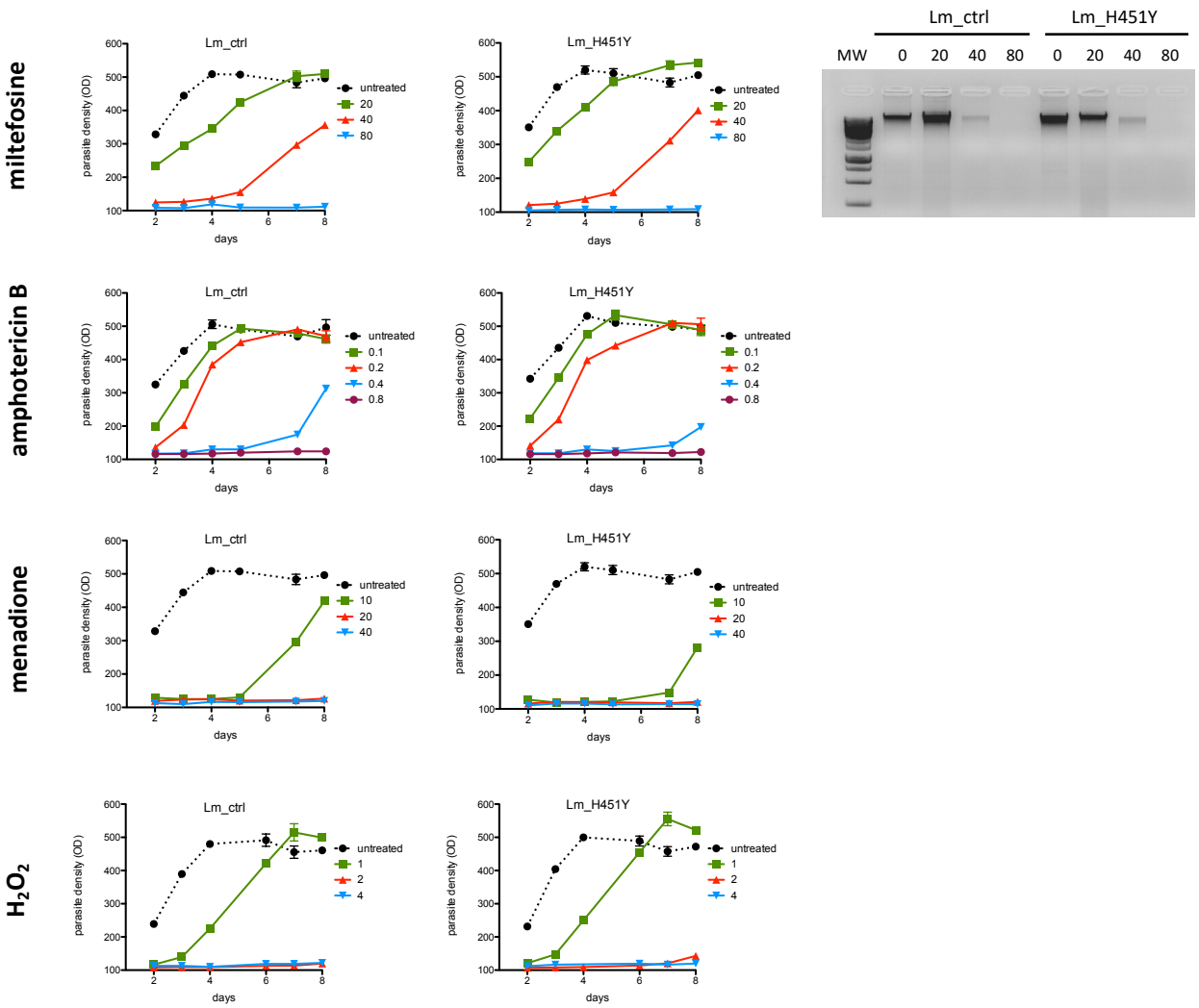

Fig. S3. Growth kinetics of Lm_ctrl and Lm_H451Y parasites exposed to different drugs that induce ROS formation. Similarly to the experiments presented in Fig. 3d, parasites were seeded at 4.10^6 parasites/mL and incubated with cytocidal concentrations of miltefosine (20, 40, 80 µM), amphotericin B (0.1, 0.2, 0.4, 0.8 µM) or menadione (10, 20, 40 µM). Parasite density was determined daily by OD measurement. For H_2O_2, parasites were incubated with 1, 2, or 4 mM H_2O_2 for 1h, then washed and resuspended in fresh medium. The integrity of genomic DNA extracted from Lm_ctrl and Lm_H451Y cultures exposed to 20, 40 or 80 µM miltefosine for three days was analysed as described in Fig. 3g.